Prediction of Secondary Flows in Non-Circular Ducts Using the Radial Functions Method

Prediction of Secondary Flows in Non-Circular Ducts Using the Radial Functions Method

Iván D. López[1,2], Lori T. Holmes[1] and Tim A. Osswald[1]
(1) Polymer Engineering Center, University of Wisconsin-Madison
(2) Plastic and Rubber Institute (ICIPC), Medellin-Colombia

Abstract

The flow through non-circular tubes is simulated using the radial functions method (RFM). The Giesekus model is considered to reproduce viscoelastic effects. RFM is a meshless technique that does not require homogeneous grid points. The technique successfully modeled the flow through square tubes reproducing the secondary flows observed experimentally by other researchers. Furthermore, the results are in agreement with finite element and finite volume numerical approaches. When considering high Weissenberg numbers, meshless techniques avoid the limitations of typical methods using meshes, such as capturing steep stress gradients at sudden changes in geometry.

Introduction

For two decades, researchers have been working on the modeling of viscoelastic flows in 3D geometries. Although some complex flows have been successfully simulated, they are still limited to low Weissenberg number (We) values while requiring high computational times. Meshless techniques such as the Radial Functions Method (RFM) offer a novel and an interesting approach to study viscoelasticity. In particular, this work is focused on the prediction of secondary flows caused by viscoelastic effects in straight non-circular ducts, which are typical in geometries of extrusion dies.

The magnitude of the secondary flows is usually many orders lower than the axial flow. However, they may produce significant impacts in practical applications. Syrjala [15] demonstrates using the finite element method that secondary flows can affect drastically the temperature distribution in low-viscous flows. Dooley [3,4] investigates how the presence of secondary flows generates elastic layer rearrangement in multilayer coextrusion, which results in layer thickness variations.

Yue et al. [17] summarize the publications that have reported results of simulations of secondary flows in noncircular ducts. Those publications include the work of Debbaut [2] and Dooley [3,4] using the Giesekus model with finite elements, and the work of Tanoue et al. [16] predicting secondary flows with the PTT model. Experimentally, several authors have observed recirculations in elliptic pipes [6] and square cross-section ducts [3,4].

Only in the last six years the applications of meshless techniques with radial basis functions have been extended to the simulation of non-Newtonian flows. Those works includes the publications of Er-Riani et al. [5], López, Osswald et al. [8-11,13], Mai-Dui and Tanner [12], Bernal and Kindelan [1]. The viscoelastic study with radial basis functions is reduced to the work of Mai-Dui and Tanner [12], who simulated the axisymmetric flow in tubes using Newtonian, power-law, and Oldroyd-B models and flows through straight ducts using the Criminale–Ericksen–Filbey (CEF) model with a stream and vorticity approach. That work represents an important step in the solution of viscoelastic flows using meshfree methods. However, the solution of a CEF model does not guarantee the solution of more complex models such as Phan Thien Tanner (PTT) and Giesekus models, and the stream and vorticity approach may not work for three-dimensional solutions. In the present work, the solution with RFM is formulated for a general differential constitutive equation, using in particular the Giesekus model, and compared with results observed experimentally and solved numerically by other researchers.

Modeling and Numerical Implementation

The secondary flows of viscoelastic fluids in noncircular straight ducts are orthogonal to the main direction of the flow. They are caused by the stress tensor components in the transverse plan. The duct geometry plays an important role in the generation of recirculations, wherefore secondary flows are only formed in non-axissymmetric cross-sections . A detailed description of the mechanisms that generate secondary flows is presented by Yue et al. [17].

In order to model viscoelasticity, the stress, τ, is split into a purely viscous component, τ_N, and an extra-stress, τ_v which contains the elastic components. This stress split has an important impact on the numerical stability of the governing equations [14]. The total stress can be written as

$$\boldsymbol{\tau} = \boldsymbol{\tau}_{\mathbf{v}} + \boldsymbol{\tau}_{\mathbf{N}} \qquad (1)$$

Neglecting inertia and gravitational effects, the momentum equation can be written as,

$$0 = -\nabla p + \nabla \cdot \boldsymbol{\tau}_{\mathbf{N}} + \nabla \cdot \boldsymbol{\tau}_{\mathbf{v}} \qquad (2)$$

The constitutive equation for τ_N is given by

$$\boldsymbol{\tau}_{\mathbf{N}} = s\eta\dot{\boldsymbol{\gamma}} \qquad (3)$$

where *s* is a weight factor between 0 and 1 that indicates how important is the Newtonian contribution of the stress compared to the total stress.

The viscoelastic part of the stress, τ_v can be modeled using differential or integral formulations. Differential models have been traditionally the choice to simulate polymeric fluids. The general form of a differential viscoelastic model is given by

$$Y\boldsymbol{\tau}_{\mathbf{v}} + \lambda_1\boldsymbol{\tau}_{\mathbf{v}_{(1)}} + \lambda_2\{\dot{\boldsymbol{\gamma}} \cdot \boldsymbol{\tau}_{\mathbf{v}} + \boldsymbol{\tau}_{\mathbf{v}} \cdot \dot{\boldsymbol{\gamma}}\} + \lambda_3\{\boldsymbol{\tau}_{\mathbf{v}} \cdot \boldsymbol{\tau}_{\mathbf{v}}\} = (1-s)\eta\dot{\boldsymbol{\gamma}} \qquad (4)$$

where $\tau_{v(1)}$ is the convected derivative of the deviatoric stress and it is defined as

$$\boldsymbol{\tau}_{v_{(1)}} = \frac{D\boldsymbol{\tau}_{\mathbf{v}}}{Dt} - [(\nabla\mathbf{u})^T \cdot \boldsymbol{\tau}_{\mathbf{v}} + \boldsymbol{\tau}_{\mathbf{v}} \cdot (\nabla\mathbf{u})] \qquad (5)$$

Depending on the definition of the parameters Y, λ_1, λ_2 and λ_3 the viscoelastic model changes [13]. The parameter definitions for the most common viscoelastic constitutive models are listed in Table 1.

Table 1: Parameter definitions for the viscoelastic constitutive models

Model	Y	λ_1	λ_2	λ_3
Generalized Newtonian	1	0	0	0
Upper convected Maxwell	1	λ	0	0
White-Metzner	1	$\lambda(\dot{\gamma})$	0	0
Phan-Thien Tanner-1	$e^{\left(-\varepsilon\left(\frac{\lambda}{(1-s)\eta}\right)\mathrm{tr}\boldsymbol{\tau}\right)}$	λ	$\frac{1}{2}\xi\lambda$	0
Phan-Thien Tanner-2	$1-\varepsilon\left(\frac{\lambda}{(1-s)\eta}\right)\mathrm{tr}\boldsymbol{\tau}$	λ	$\frac{1}{2}\xi\lambda$	0
Giesekus	1	λ	0	$-(\alpha_g\lambda/\eta_0)$

The numerical implementation is based on the Radial Function Method (RFM) which was introduced by Kansa [6]. This method allows the approximation of a field variable in a continuous space by a linear combination of interpolation coefficients and Radial Basis Functions (RBF). For example, pressure can be written as:

$$p_i = \sum_{j=1}^{Np} \phi_p(r_{ij})\beta_j \qquad (5)$$

where $Beta_j$ is the interpolation coefficient rij is the distance between the nodes i and j and $theta_p(r_{ij})$ represents the RBF to interpolate unknown fields. In this work the Thin Plate Spline (TPS) is used as the RBF.

In a similar way, the velocity components and the stress tensor components can be rewritten as

$$u_{x_i} = \sum_{j=1}^{N} \phi_u(r_{ij})\iota_j \qquad (6)$$

$$u_{y_i} = \sum_{j=1}^{N} \phi_u(r_{ij})\varpi_j \qquad (7)$$

$$u_{z_i} = \sum_{j=1}^{N} \phi_u(r_{ij})\chi_j \qquad (8)$$

$$\tau_{v_{xx_i}} = \sum_{j=1}^{N} \phi_\tau(r_{ij})\rho_j \qquad (9)$$

$$\tau_{v_{xy_i}} = \sum_{j=1}^{N} \phi_\tau(r_{ij})\upsilon_j \qquad (10)$$

$$\tau_{v_{yy_i}} = \sum_{j=1}^{N} \phi_\tau(r_{ij})\varphi_j \qquad (11)$$

$$\tau_{v_{xz_i}} = \sum_{j=1}^{N} \phi_\tau(r_{ij})\psi_j \qquad (12)$$

$$\tau_{v_{yz_i}} = \sum_{j=1}^{N} \phi_\tau(r_{ij})\kappa_j \qquad (13)$$

$$\tau_{v_{zz_i}} = \sum_{j=1}^{N} \phi_\tau(r_{ij})\varepsilon_j \qquad (14)$$

Let us consider a viscoelastic fluid that flows through a straight noncircular duct. Figure 1 schematically depicts the geometry of a square duct. The main flow direction is defined by the z-axis and the secondary recirculations occur in the xy plane. The section is constant along the duct and the flow is assumed fully developed. Therefore, we can assume that the pressure drop, ΔP/L and velocity and stress tensor components are constant in the main flow direction. This allows the 2-1/2D RFM formulation (a 3D flow where the velocity field does not change in the z-direction), requiring only the cross-section of the channel to model the flow. In that kind of geometry we can assume that the velocity field does not change in the z-direction. Based on this assumption, and using τ_N as defined in (3), the x- component of the momentum equation (2) is simplified as

$$0 = -\frac{\partial p_i}{\partial x} + s\left[\eta_i \nabla^2 u_{x_i} + 2\frac{\partial \eta_i}{\partial x}\frac{\partial u_{x_i}}{\partial x} + \frac{\partial \eta_i}{\partial y}\left(\frac{\partial u_{x_i}}{\partial y} + \frac{\partial u_{y_i}}{\partial x}\right)\right] + \frac{\partial \tau_{v_{xx_i}}}{\partial x} + \frac{\partial \tau_{v_{xy_i}}}{\partial y} \qquad (15)$$

The above equation can be approximated with RBFs by using the definitions of eqs. (6-14):

$$
\begin{aligned}
&s\sum_{j=1}^{N}\left[\begin{array}{c}-\eta_i\nabla^2\phi_u(r_{ij})\\ -\dfrac{\partial\phi_u(r_{ij})}{\partial r}\left(2\dfrac{\partial\eta_i}{\partial x}\dfrac{\partial r_{ij}}{\partial x}+\dfrac{\partial\eta_i}{\partial y}\dfrac{\partial r_{ij}}{\partial y}\right)\end{array}\right]\iota_j + \\
&\quad s\sum_{j=1}^{N}\left[-\frac{\partial\phi_u(r_{ij})}{\partial r}\frac{\partial\eta_i}{\partial y}\frac{\partial r_{ij}}{\partial x}\right]\varpi_j + \\
&+\sum_{j=1}^{N_p}\left[\frac{\partial\phi_p(r_{ij})}{\partial r}\frac{\partial r_{ij}}{\partial x}\right]\beta_j-\sum_{j=1}^{N}\left[\frac{\partial\phi_\tau(r_{ij})}{\partial r}\frac{\partial r_{ij}}{\partial x}\right]\rho_j \\
&\quad -\sum_{j=1}^{N}\left[\frac{\partial\phi_\tau(r_{ij})}{\partial r}\frac{\partial r_{ij}}{\partial y}\right]\upsilon_j=0
\end{aligned}
\tag{16}
$$

The same procedure should be followed for the other two components of the momentum equations, the continuity equation and the constitutive equation presented in (4). The values for the pressure, velocity and stress fields can be obtained by applying the boundary conditions and solving for the interpolation coefficieints. The stress and rate of deformation tensors of (4) are unkonwn, requiring an iteration process which starts using a Newtonian solution.

Results

The present work considers the processing conditions and material properties used by Dooley in his work [3,4], taking advantage of the possibility of verifying the results with experimental measurements and results delivered by other numerical methods.

Square Duct

The first geometry considered is a straight square duct as the depicted in Figure 1. The material properties and processing conditions listed in Table 2 are used. Those conditions are the same used by Dooley in his experiments and numerical simulations with polystyrene. The Giesekus equation is considered to model the viscoelastic effect.

Table 2: Processing conditions and material properties used by Dooley to model the secondary flows in a square duct for polystyrene

Parameter	Value
H	1cm
$\Delta P/L$	20MPa/m
λ	0.06s
η	8000Pa-s
s	0
α_g	0.8

Four hundred nodes uniformly distributed are considered to approach the solution. When a simulation was performed using the upper convected Maxwell model ($\alpha_g = 0$), no secondary flows were observed. This is expected since the Maxwell model does not predict the second normal stress difference which causes the recirculation. Figure 2 compares the secondary flows delivered by RFM using Giesekus model with the FEM simulation and the experimental observation of Dooley's work. The RFM solution is overlapped with Dooley's observations and simulations in Fig. 3. RFM clearly predicts the same flow pattern obtained in Dooley's work, with a good agreement in the estimation of the recirculation center locations. The secondary flows have 1% the order of magnitude of the main flow, which coincides with Dooley's FEM results.

The RFM predictions of the stress tensor components and pressure variations in the transversal section are depicted in Fig.4. The theoretical symmetry of the system is correctly described by RFM. The stress results are smooth and free of oscillations. Some oscillations can be appreciated in the pressure solution; however, they do not seem to compromise the accuracy and smoothness of velocity and stress tensor estimations.

Teardrop Duct

A teardrop shape duct approximates the geometry used in many extrusion die distribution systems. The generation of secondary flows in distribution manifolds may have important effects in the coextrusion of multilayer films as discussed by Dooley [3].

The same material properties and processing conditions used for the square duct were considered (Table 2). The geometry and dimensions of the teardrop were defined in such as way that the volumetric flow rate was equal to that of the square duct case. Figure 5 shows the node distribution used for the simulation. Only a half of the geometry was considered taking advantage of the symmetry. Three hundred collocation nodes were used for the solution.

Figure 6 compares the secondary flows delivered by RFM with the FEM simulation and the experimental observation of Dooley's work. The numerical solutions render the same secondary flow patterns observed experimentally, predicting six vortices where the strongest secondary flow is along the longest duct direction.

Conclusions

RFM offers a novel, simplified approach to model viscoelasticiy. RFM has the potential to solve for geometries with a high degree of complexity. The cost benefit of RFM is to use as few nodes as possible while continuing to increase We.

Nonlinear viscoelasticity was modeled using RFM. A general formulation that includes Giesekus, Phan Thien Tanner and Upper Convective Maxwell models was implemented for two-dimensional flows and flows that consider the three components of velocity but neglecting changes in the z-direction. RFM was able to reproduce accurately the secondary flows in straight noncircular ducts experimentally observed and numerically predicted in Dooley's work [3,4].

Future Work

The solution for viscoelastic fluids using RFM should be extended to higher Weissenberg number (We) values in order to reproduce actual extrusion conditions. This can be achieved using relaxation strategies during the iteration process.

A natural step is to proceed with the simulation of fully three-dimensional viscoelastic flows, and use the implementation described in this paper, to study the elastic effect in extrusion dies.

References

[1] F. Bernal and M. Kindelan. “RBF meshless modeling of non-Newtonian Hele-Shaw Flow”. Engineering Analysis with Boundary Elements, 31: 863 -874, 2007.
[2] B. Debbaut and J Dooley. Secondary motions in straight and tapered channels: Experiments and threedimensional finite element simulation with a multimode differential viscoelastic model. Journal of Rheology, 43(6):1525-1545, 1999.
[3] J. Dooley. Viscoelastic flow effect in multilayer polymer coextrusion. PhD thesis, Tecnhische Universiteit Eindhoven, 2002.
[4] J. Dooley and L Schkopau. Viscous and Elastic Effects in Polymer Coextrusion. Journal of Plastic Film and Sheeting, 19(2):111-122, 2003.
[5] M. Er-Riani, A. Naji, A. Nouar, and O. SeroGuillaume. Multiquadrics method for Couette flow of a yield-stress fluid under imposed torques. International Workshop on MeshFree Methods Proceedings, 2003.
[6] H. Giesekus. Sekundrstrmungen in viskoelastischen flssigkeiten bei stationrer und periodischer bewegung. Rheol. Acta 4, page 85101, 1965
[7] E. J. Kansa. “Multiquadrics - a scattered data approximation scheme with applications to computational fluid-dynamics .1.” Computers & Mathematics with Applications, 19(8-9):127- 145, 1990.
[8] I. D. López, O. Estrada, and T. Osswald. “Modeling and simulation of polymer processing using the radial functions method”. Ak Zeitschrift Kunststofftechnik, 2007.
[9] I. D. López, O. Estrada, Noriega M. D. P., and W. F Flórez. “Collocation method solution with radial basis functions of the 2d energy equation”. ANTEC, Annual Technical Conference Proceedings, 2005.
[10] I. D. López, S. Hoffman, A. Bednar, and T. Osswald. “Filling simulation and temperature prediction in hot runner systems”. ANTEC, Annual Technical Conference Proceedings, 2008.
[11] I. D. López, F. Klaiber, and T. Osswald. “Analysis of viscous heating effect in a pressure slit rheometer using the radial functions method (RFM)”. ANTEC, Annual Technical Conference Proceedings, 2006.

[12] N. Mai-Duy and R. I. Tarmer. "Computing nonNewtonian fluid flow with radial basis function networks". International Journal for Numerical Methods in Fluids, 48: 1309- 1336, 2005.
[13] T. Osswald, López I.D. Hernandez, J.P, and O. Estrada. Polymer Processing Modeling and Simulation, Chapter 11: "Radial Function Method". Hanser, 2006.
[14] J.F.T. Pittman and Tucker III C. L. Fundamentals of Computer Modeling for Polymer Processing. Hanser Publishers, 1989.
[15] S. Syrjala, Laminar flow of viscoelastic fluids in rectangular ducts with heat transfer: A finite element analysis. International Communications in Heat and Mass Transfer, 25(2):191-204, 1998.
[16] S. Tanoue, T. Naganawa, and Y. Iemoto. Quasithree-dimensional simulation of viscoelastic flow through a straight channel with a square cross section. Nihon Reoroji Gakkaishi, 34(2):105-113, 2006.
[17] P. Yue, J. Dooley, and J.J. Feng. A general criterion for viscoelastic secondary flow in pipes of noncircular cross section. Journal of Rheology, 52(1):315-332, 2008.

Key Words: Viscoelasticity, Giesekus model, Radial Function Method (RFM), Non-circular tubes, Secondary flows, Meshless method.

Figures

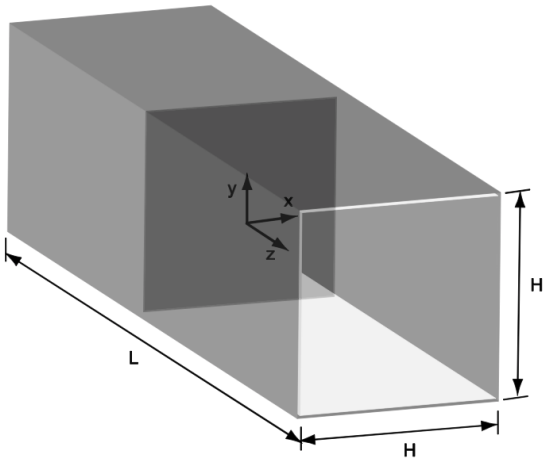

Figure 1: Schematic diagram of a square duct

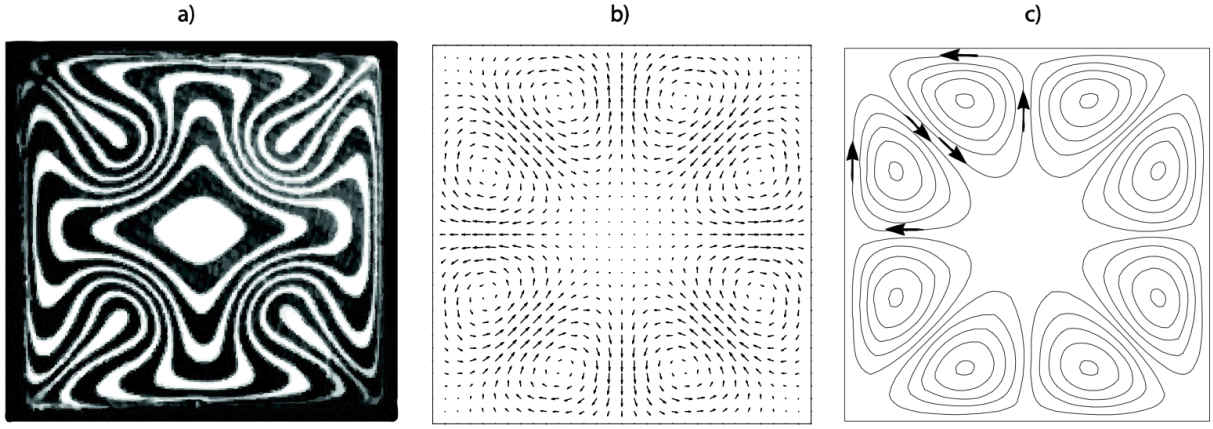

Figure 2. Polystyrene Secondary flows in a square channel: a)Experimental Results. b) RFM prediction. c)FEM prediction

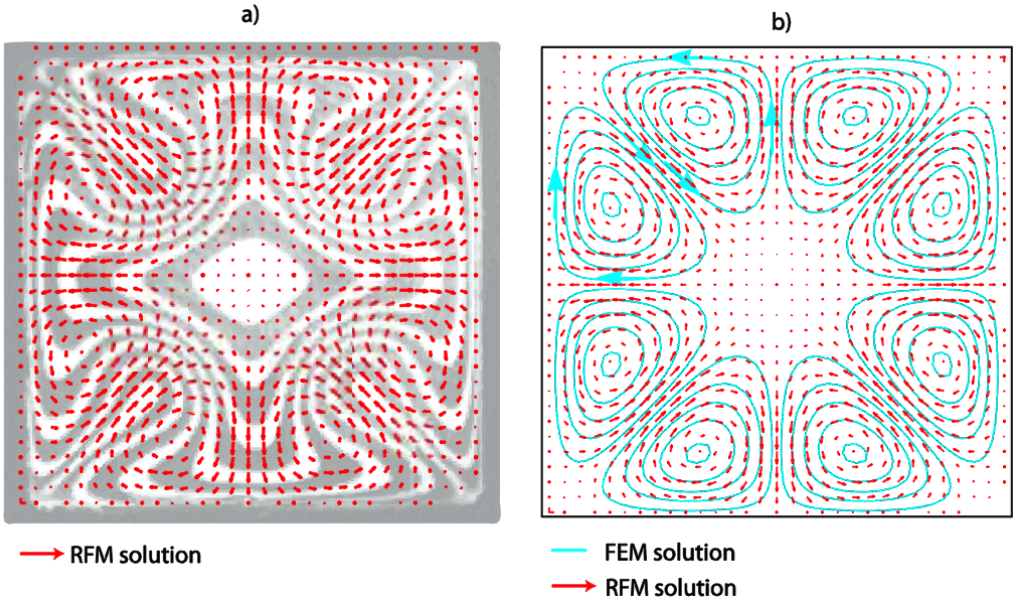

Figure 3: Comparison of the prediction of secondary flows in a square channel of RFM with: a)Experimental Results. b) FEM results

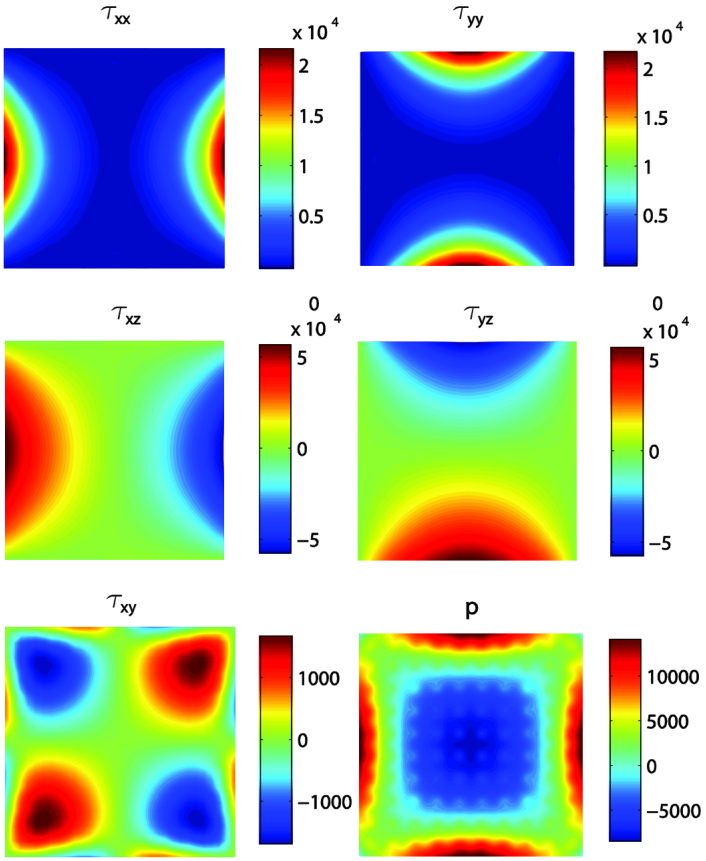

Figure 4: Stress tensor components and pressure values (Pa) for a square duct flow prediction

Figure 5. Node distribution for the RFM modelling of secondary flows in a teardrop shape duct.

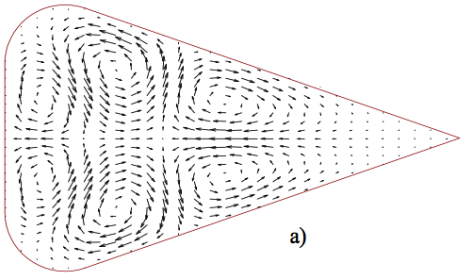

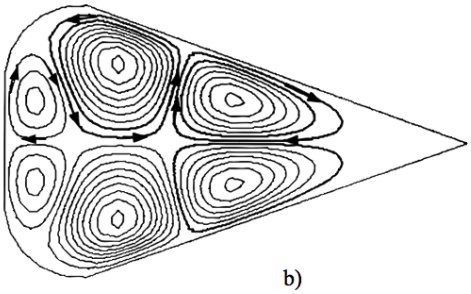

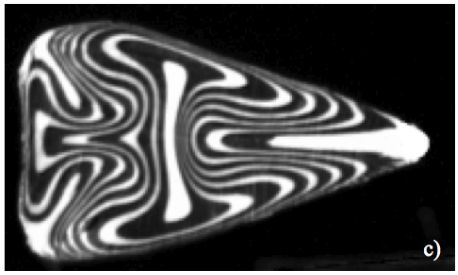

Figure 6. Polystyrene Secondary flows in a teardrop shape channel: a) RFM prediction. b) Dooley´s FEM pediction c)Dooley´s experimental observation

Return to Paper of the Month.